Differential cross sections and analyzing powers for neutron elastic scattering from ^{89}Y between 8 and 17 MeV

G. M. Honoré,* R. S. Pedroni, C. R. Howell, H. G. Pfützner, R. C. Byrd,†
G. Tungate,‡ and R. L. Walter
Department of Physics, Duke University, Durham, North Carolina 27706
and Triangle Universities Nuclear Laboratory, Duke Station, North Carolina 27706
(Received 28 April 1986)

Differential cross sections and analyzing powers for neutron elastic scattering from ^{89}Y have been measured at energies from 8 to 17 MeV using a neutron time-of-flight facility. The data have been analyzed with the spherical optical model and excellent representations are achieved at all energies with the derived optical potential parameters, which were constrained to vary linearly with energy. Comparisons have been made to two previously reported global spherical optical models as well.

I. INTRODUCTION

The program of measuring differential cross sections and analyzing powers for neutron scattering at Triangle Universities Nuclear Laboratory (TUNL) has been expanded to include the nucleus ^{89}Y. In the present paper we report experimental and spherical optical model (SOM) investigations of elastic scattering of neutrons from ^{89}Y in the energy region from 8 to 17 MeV. This is an important energy region for investigating neutron-nucleus direct-reaction model calculations. Considerable work has already been performed in the area of SOM studies by Rapaport *et al.*[1,2] and, more recently, by Walter and Guss.[3] Their global parametrizations of phenomenological optical models have been quite successful in describing nucleon-nucleus scattering data for many spherical and deformed nuclei in and beyond the energy range of the present investigation.

We have been interested in obtaining more data for nucleon-nucleus elastic scattering in the mass region near $A=90$, and specifically near the magic number $N=50$. Our purpose is, in part, to supplement the existing neutron-scattering data base for medium- to heavy-weight nuclei for incident energies between 8 and 20 MeV. Recent measurements for ^{89}Y have been reported at 14.6 MeV by Hansen *et al.*[4] at Lawrence Livermore National Laboratory (LLNL) and at 11.0 MeV by Yiming *et al.*[5] at Ohio University; unfortunately, their studies focused only on data at a single energy. Prior to the present measurements, no analyzing power data for neutron elastic scattering have been available for ^{89}Y; consequently, these previous analyses have employed spin-orbit parametrizations based on scattering studies for other nuclei. In the present work differential cross sections $\sigma(\theta)$ are reported for elastic scattering of neutrons from ^{89}Y at incident energies 7.96, 9.95, 11.94, 13.93, and 16.93 MeV. In addition, analyzing powers for this nucleus have been measured at 9.95, 13.93, and 16.93 MeV.

Since in the present work only neutron elastic-scattering data have been obtained for ^{89}Y, the SOM was the main tool used for analyzing these data. Our purposes were twofold. First, we wished to find a set of parameters that vary systematically with energy in order to test the applicability of the SOM to ^{89}Y. With success at this stage, the model can be used for a more general phenomenological description of scattering from this nucleus. Second, it was believed that the analysis would provide significant new information, in addition to the new data, for improving the parametrization of the global SOM being developed at TUNL.[3] In this context the data also provide an interesting test of other existing SOM global parameter sets.

For completeness, a level diagram of ^{89}Y is given in Fig. 1. The adjacent neutron closed-shell nuclei ^{88}Sr and ^{90}Zr, both with $N=50$, are known to have low-lying states of collective character. The nucleus ^{89}Y also has 50 neutrons but, in addition, an unpaired $2p_{1/2}$ proton; experimental investigations of the structure of ^{89}Y have been made using the (p,p') reaction (for example, that of Benenson *et al.*[6]), and thirteen excited states have been observed below 3.2 MeV. Several theoretical studies also exist, in which the level structure of this nucleus is successfully calculated using the shell model.[7–9]

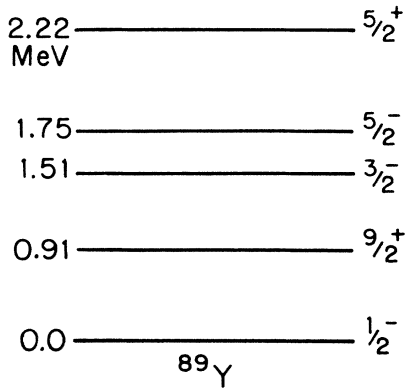

FIG. 1. The low-lying levels of ^{89}Y.

II. EXPERIMENT

A. Differential cross sections

The differential cross sections were measured using pulsed-beam time-of-flight (TOF) methods. The experimental arrangement has been described in earlier papers.[10,11] Briefly, a deuteron beam is pulsed and then accelerated with the TUNL FN tandem van de Graaff, producing a pulsed neutron beam via the ^{2}H(d,n)^{3}He reaction. Neutrons emitted at 0° reaction angle scatter from a cylindrical target, 2.54 cm in height and 1.91 cm in diameter, composed of 32.9 g of elemental yttrium, which is estimated to be 99.5% ^{89}Y. The remaining 0.5% is believed to be comprised of light elements such as oxygen. Scattered neutrons are detected by two heavily shielded liquid organic scintillators at flight paths of 4 and 6 m, respectively. Standard TOF electronics are used, as described in Ref. 10, and γ-ray events are excluded by pulse-shape discrimination methods. A third neutron detector views the ^{2}H(d,n)^{3}He reaction from above the reaction plane to monitor the incident flux.

Examples of TOF spectra are shown in Fig. 2. Time-of-flight increases from right to left. The peak at far right is due to elastic scattering from ^{89}Y. Spectra obtained with the sample removed are subtracted from "sample-in" spectra to remove the sample-uncorrelated background. The resulting difference spectra, illustrated in Fig. 2, are then normalized to the yields in a flux-monitor detector in order to obtain relative angular distributions at each energy. The angular distributions are converted to absolute cross sections by normalizing to yields obtained from neutron scattering from hydrogen in a polyethylene target of known composition, and to published n-p scattering cross sections.[12]

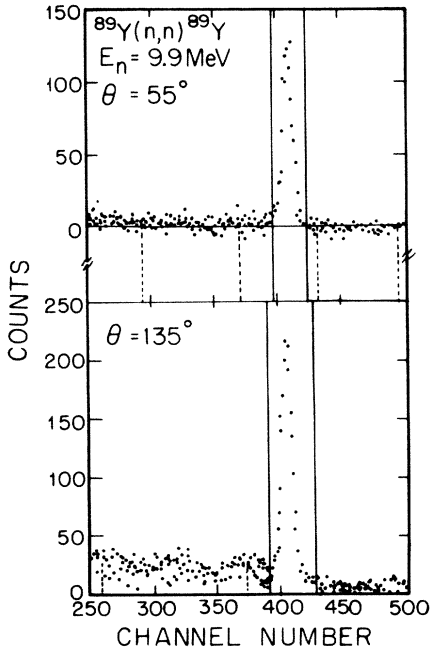

FIG. 2. Time-of-flight spectra for the elastic scattering of 9.9 MeV unpolarized neutrons from yttrium through laboratory angles $\theta=55°$ and 135°. Time increases from right to left. The figure indicates the windows used to extract the cross sections for elastic scattering.

B. Analyzing powers

The TOF measurements of analyzing powers $A_y(\theta)$ were conducted in the same target room as the $\sigma(\theta)$ measurements, using the same heavily shielded detectors. Because the experimental arrangement has been described in great detail in Ref. 11, only a summary will be presented here. A pulsed, polarized deuteron beam from the TUNL Lamb-shift polarized ion source is used to produce polarized neutrons through the polarization-transfer reaction ^{2}H($\vec{d},\vec{n}$)^{3}He at $\theta=0°$. The polarization of the deuteron beam, as measured by the quench-ratio method,[13] was typically 70%, giving a neutron beam with a polarization of about 63%. All $A_y(\theta)$ measurements were made with left and right detectors set at equal reaction angles, using the "two-detector, spin-flip" method,[14] in order to minimize instrumental asymmetries. Measurements were made in 10° increments from 30° to 150°, and in smaller steps for scattering angles of less than 30°. The counting statistics obtained with polarized neutrons were slightly worse than those in Fig. 2.

C. Date reduction and presentation

The distributions of $\sigma(\theta)$ reported here were measured in 5° steps over a typical range of 25°–160°. The TOF spectra were analyzed using computer codes developed at TUNL. In general, the quality of the spectra was not sufficient to permit the extraction of any inelastic-scattering data. Furthermore, the TOF spectrometer did not resolve the cluster of low-lying states in this nucleus.

Corrections were made to both $\sigma(\theta)$ and $A_y(\theta)$ data for the effects of finite geometry and multiple scattering, using the TUNL Monte Carlo codes EFFIGY for correcting[15] cross sections and JANE for correcting[16] the analyzing powers. The final results are shown in the center-of-mass system in Fig. 3. The $\sigma(\theta)$ data have relative uncertain-

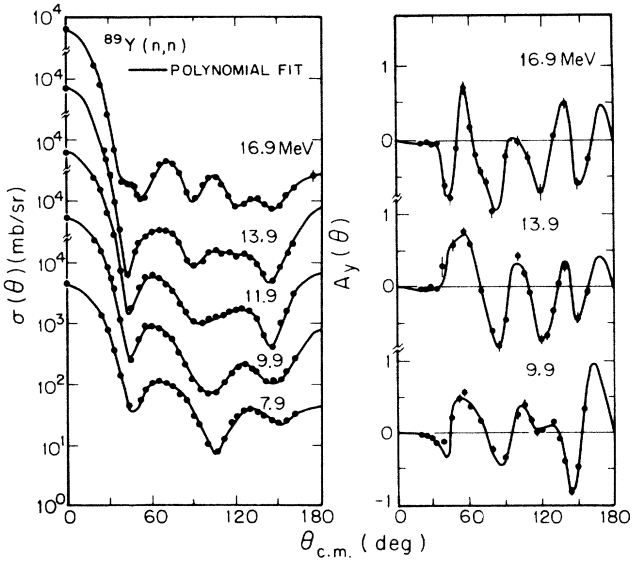

FIG. 3. Differential cross sections and analyzing powers for elastic scattering of neutrons from ^{89}Y. The curves are derived from expansions in Legendre polynomials.

ties between 2.5% and 6%, and an absolute normalization uncertainty of about 3%. Uncertainties are not shown when smaller than the symbol size. The $\sigma(\theta)$ data were fitted with expansions in Legendre polynomials (solid curves in Fig. 3) using our program MACRO, which employs statistical criteria to determine the order of the fits.

The solid curves accompanying the $A_y(\theta)$ data in Fig. 3 are derived from associated Legendre polynomial fits to the product $\sigma(\theta)A_y(\theta)$. The final data have uncertainties ranging from less than ± 0.02 at forward angles to about ± 0.08 at some backward angles. The error bars include all uncertainties, except a uniform scale factor of about ± 0.03, attributable to uncertainties in the quench-ratio measurement and in the $^2\mathrm{H}(\vec{d},\vec{n})^3\mathrm{He}$ polarization-transfer coefficient. Tabulations of all the data have been transmitted to the National Nuclear Data Center at Brookhaven National Laboratory.

III. SPHERICAL OPTICAL MODEL PREDICTIONS

A. Introduction

Since ^{89}Y can be assumed to be nearly spherical, it is a good candidate for an analysis with the spherical optical model (SOM). We define the optical model potential to be

$$U(r) = -Vf(r,R_R,a_R) - iW_v f(r,R_v,a_v) + 4ia_d W_d \frac{df}{dr}(r,R_d,a_d) + 2\lambda_\pi^2 \left[V_{\mathrm{SO}} \frac{df}{dr}(r,R_{\mathrm{SO}},a_{\mathrm{SO}}) \mathbf{l}\cdot\mathbf{s} + iW_{\mathrm{SO}} \frac{df}{dr}(r,R_{W_{\mathrm{SO}}},a_{W_{\mathrm{SO}}}) \mathbf{l}\cdot\mathbf{s} \right],$$

where the form factors $f(r,R_i,a_i)$ are Woods-Saxon functions defined as

$$f(r,R_i,a_i) = \{1+\exp[(r-R_i)/a_i]\}^{-1} .$$

All the TUNL $\sigma(\theta)$ and $A_y(\theta)$ data from 8 to 17 MeV were combined to form a single data set. Neutron total cross section σ_T data obtained from Foster and Glasgow[17] were included in the set, and predictions of this observable were also made at each energy. These data were important for determining reasonable values for the absorptive potentials.

All calculations were performed using the SOM search code GENOA, originally obtained from Perey of Oak Ridge National Laboratory. The version of GENOA used in this work has been modified[18] to calculate the Mott-Schwinger interaction between the magnetic moment of the incident neutron and the Coulomb field of the nucleus. This interaction is known to have a significant effect on neutron analyzing powers, particularly in the forward-angle region.

The weighting of $A_y(\theta)$ in the parameter searches was adjusted to be twice that of $\sigma(\theta)$. This was done for the following reasons: First, because there were many more cross section data than analyzing power data, the cross sections would normally exert a greater influence on the searches. Second, the $\sigma(\theta)$ data generally have smaller uncertainties than do the $A_y(\theta)$ data, and so would be more heavily weighted for this reason as well. Lastly, part of the purpose of this ^{89}Y study is to explore the spin-orbit (SO) potential, including the behavior of the imaginary spin-orbit potential W_{SO}. This latter part of the potential is more sensitive to the analyzing power data.

B. Single-energy representation of data

Searches were made first at individual energies to establish a group of "best-fit" parameters. Starting parameters for the SOM searches were taken from an early version of a TUNL global SOM parameter set,[19] derived from searches on cross section and analyzing power data over a wide energy range, for nuclei ranging from ^{40}Ca to ^{208}Pb, but not including nuclei in the region of ^{89}Y because no analyzing power data were available there. In fact, the starting parameters give a fairly good representation of the data. A search scheme similar to that described by Rapaport[2] was used. As is usual in optical model analyses, the goodness of fit was determined by the chi-squared per point χ_N^2, hereafter symbolized by χ^2. The strengths of the central potentials V_R, W_d, and W_v were searched first. These strengths were then searched again, along with the real diffuseness a_R and the imaginary radii r_d and r_v. The potential strengths were then searched a third time in conjunction with all their associated geometries. Searches of the spin-orbit strengths and geometries followed. Parameters were restricted in some cases to prevent unphysical results and to avoid certain known ambiguities,[20] such as those between V_R and r_R and between W_d and a_d.

Because of the relatively limited energy range of the available data, it was decided to constrain all geometrical parameters to be independent of energy. Therefore, the next step was to calculate mean values of the geometries obtained in the best-fit searches described above. These average geometries were then inserted and the potential strengths were searched again at each energy individually. At the conclusion of this phase we had the best estimate of potential strengths at all five energies and a geometry set common to all energies.

C. Energy-dependent representation of data

The final determination of the SOM representation of ^{89}Y was to establish appropriate energy dependences for the potential strengths. The strengths were assumed to have simple variations with energy, and searches for the optimum dependences were made, keeping the geometries fixed at the average values. This gave a representation of the data that is both more compact and systematic than the single-energy descriptions. The potential strengths vary linearly with energy: V_R and V_{SO} are linearly de-

creasing; W_d increases linearly up to a critical energy $E_c = 10$ MeV and decreases linearly thereafter. For energies above E_c we identified the need for an imaginary volume term, and have included one with a linear energy dependence: W_v increases linearly above E_c. The imaginary surface term W_d is also constrained to be continuous at the critical energy E_c. The functional dependences of the potential strengths (in MeV) are summarized as follows:

$$V_R = V_{0R} - \alpha_R E \ ,$$

$$W_v = 0 \quad (E < E_c) \ ,$$

$$W_v = W_{0v} + \alpha_v E \quad (E \geq E_c) \ ,$$

$$W_d = W_{0d} + \alpha_d E \quad (E \leq E_c) \ ,$$

$$W_d = W_{0d'} - \alpha'_d E \quad (E \geq E_c) \ ,$$

$$V_{SO} = V_{0SO} - \alpha_{SO} E \ ,$$

$$W_{SO} = W_{0SO} - \alpha_{W_{SO}} E \ .$$

The quality of the fits with this energy-dependent model is quite high; this model is nearly as successful as the best fits in describing the data. The parametrization of this constrained model is summarized in Table I, along with the RKF and WG (Rapaport-Kulkarni-Finlay and Walter-Guss) representations. One should note that the well depths and geometry parameters of the present work are similar to those of the others. The main difference with the RKF representation is in the SO term: our data require a smaller SO diffuseness and a larger SO radius than used by RKF, who adopted the values of Becchetti and Greenlees.[21]

The calculations of cross sections and analyzing powers using the parameter set of Table I are presented in Fig. 4. The large negative values in the $A_y(\theta)$ calculations near 1° are due to the Mott-Schwinger interaction.[22] Recall that neutron total cross section data were also included in the searches. The calculated total cross sections are compared to measured values in Table II (see columns 2 and 3). The quality of agreement between the data and the calculations is very good, considering the constraints on the parameters, and the uncertainties in the σ_T measurements.

The $\sigma(\theta)$ data of Hansen *et al.*[4] at 14.6 MeV and of Yiming *et al.*[5] at 11.0 MeV are shown in Fig. 5. These data are illustrated to show how they fit into the systematics of our representation; however, they were not included in the parameter searches. The calculations at 11 MeV deviate from the Ohio University data at the forward angles, but this angular distribution is the exception. Overall, the agreement of the calculations with the data is

TABLE I. Neutron + ^{89}Y SOM parameters obtained in the present and earlier works.

Parameter	Present energy-averaged analysis[a]	Estimated uncertainty[b]	Walter-Guss model	Rapaport *et al.* RKF set *A*
V_{0R} (MeV)	51.18	1.92	50.52[c]	51.38[c]
α_R	0.241	0.109	0.32	0.353
r_R (fm)	1.20	0.03	1.219	1.198
a_R (fm)	0.69	0.08	0.688	0.663
W_{0d} (MeV)	7.29 ($E \leq 9.9$ MeV)	1.54		2.698 ($E \leq 15$ MeV)
	9.07 ($E \geq 9.9$ MeV)	1.13	9.00[c]	12.71 ($E \geq 15$ MeV)
α_d	0.0			0.4 ($E \leq 15$ MeV)
	0.179 ($E \geq 9.9$ MeV)	0.07	0.157	0.39 ($E \geq 15$ MeV)
r_d (fm)	1.31	0.08	1.282	1.295
a_d (fm)	0.50	0.05	0.512	0.59
W_{0v} (MeV)	-1.75 ($E \geq 9.9$ MeV)	0.63	-0.963	-4.3 ($E \geq 15$ MeV)
a_v	0.175	0.053	0.153	0.38
r_v (fm)	1.42	0.66	1.422	1.295
a_v (fm)	0.50	0.25[d]	0.508	0.59
V_{0SO} (MeV)	6.84	1.97	6.014	6.2[e]
α_{SO}	0.033	0.017[d]	0.015	0
r_{SO} (fm)	1.14	0.17	1.103	1.01[e]
a_{SO} (fm)	0.50	0.23	0.56	0.75[e]
W_{0SO} (MeV)	0.74	0.37[d]	0.791	0
$\alpha_{W_{SO}}$	0.009	0.004[d]	0.018	0
$r_{W_{SO}}$ (fm)	1.26	0.63[d]	1.364	0
$a_{W_{SO}}$ (fm)	0.50	0.25[d]	0.632	0

[a]Potentials are valid for $7.9 \leq E \leq 16.9$ MeV, unless otherwise indicated.
[b]Uncertainties were calculated as described in Sec. III C.
[c]This value was evaluated for ^{89}Y from the global parameter set.
[d]Search reached the 50% limit (see text).
[e]Used the SO values of Becchetti and Greenlees (Ref. 21).

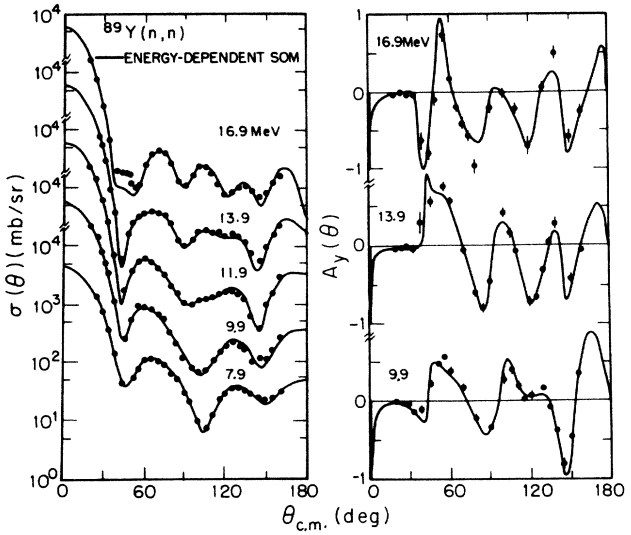

FIG. 4. Differential cross sections and analyzing powers for elastic scattering of neutrons from ^{89}Y. The curves are from calculations using the spherical optical model parameters of the present work.

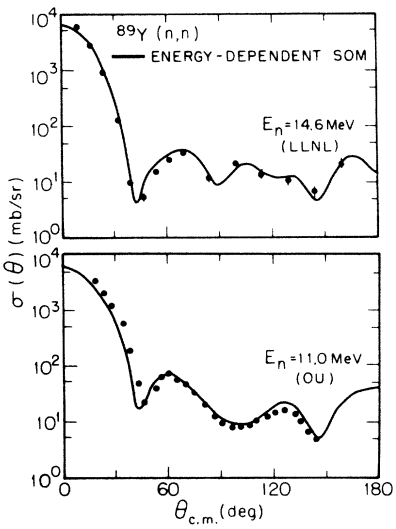

FIG. 5. Differential cross sections for elastic scattering of neutrons from ^{89}Y. The data at 11.0 MeV are from Ohio University, the data at 14.6 MeV are from Livermore National Laboratory. The curves are from calculations using the spherical optical model parameters of the present work.

excellent.

Uncertainties in the parameters of the optical model potential (OMP) were explored and estimated[23] by the following method: a parameter was varied individually, starting from its optimal value, until either the total χ^2 had doubled (relative to the value in the minimum) or the parameter had varied up or down by more than 50% of its starting value, whichever occurred *first*. Uncertainties in the OMP parameters cited in Table I were determined in this way. These values are larger than might seem intuitively desirable; however, this is due in part to the manner in which they are defined.

D. Sensitivity studies of the spin-orbit parameters

Since the ^{89}Y data between 8 and 17 MeV are well represented by the SOM calculations, we used these data to test the sensitivity of SOM predictions to variations of the parameters of the SO potential. Cross sections and analyzing powers were calculated while varying one of the three SO parameters, keeping the other two fixed at their optimal values. For each test the parameters V_{SO}, r_{SO}, and a_{SO} were incremented above and below their optimal values. Comparisons of calculations with the altered parameters to calculations with the parameters of Table I are shown for both types of data in Figs. 6–8. Based on these investigations and on studying the representations of the data set as a whole, it was possible to assign additional (empirical) uncertainties to each of the parameters in the real SO potential. The uncertainties estimated from the figures, along with the optimum values for this representation (see Table I), are as follows: $V_0^{SO}=6.8\pm0.7$ MeV, $r_{SO}=1.14\pm0.04$ fm, and $a_{SO}=0.50\pm0.07$ fm. It should be noted that the uncertainties determined in this manner are a factor of 3–4 smaller than those listed in Table I, which are based on the criterion of doubling chi-squared.

As might be expected, the calculations are most sensitive to the strength of the spin-orbit potential. The SO diffuseness appears to be the least influential of the geometrical parameters, and as such is also the least well determined. However, it is worth pointing out that since the OMP parameters are not all truly independent, the uncertainties cited here should not be considered absolute in any real sense, but rather are absolute only relative to this particular minimum in χ^2 space. It is conceivable that in another, perhaps deeper minimum in χ^2, the uncertainties on the SO parameters could be quite different.

It is also interesting to notice (see Fig. 7) that the size of the second maximum in the differential cross section near 45° in the 17 MeV angular distribution is quite sensitive to the values of r_{SO}. The inability to represent this maximum is the most obvious failing of the optimal parame-

TABLE II. Comparison of measured total cross sections to SOM calculations for ^{89}Y.

E (MeV)	Meas.[a] σ_T (mb)	Calc.[b] σ_T (mb)	Calc.[c] σ_T (mb)	Calc.[d] σ_T (mb)
17.0	3572	3581	3560	3707
14.0	3866	3912	3901	4042
12.0	4082	4137	4123	4158
10.0	4241	4280	4268	4181
8.0	4332	4252	e	4041

[a]Data obtained from Ref. 17. The uncertainties are about 60 mb.

[b]Calculations made with the parameter set of the present work.

[c]Calculations made with the parameter set of WG (Ref. 3).

[d]Calculations made with the parameter set of RKF (Refs. 1 and 2).

[e]Calculations not appropriate at this energy, since this model only applies for energies greater than 9.9 MeV.

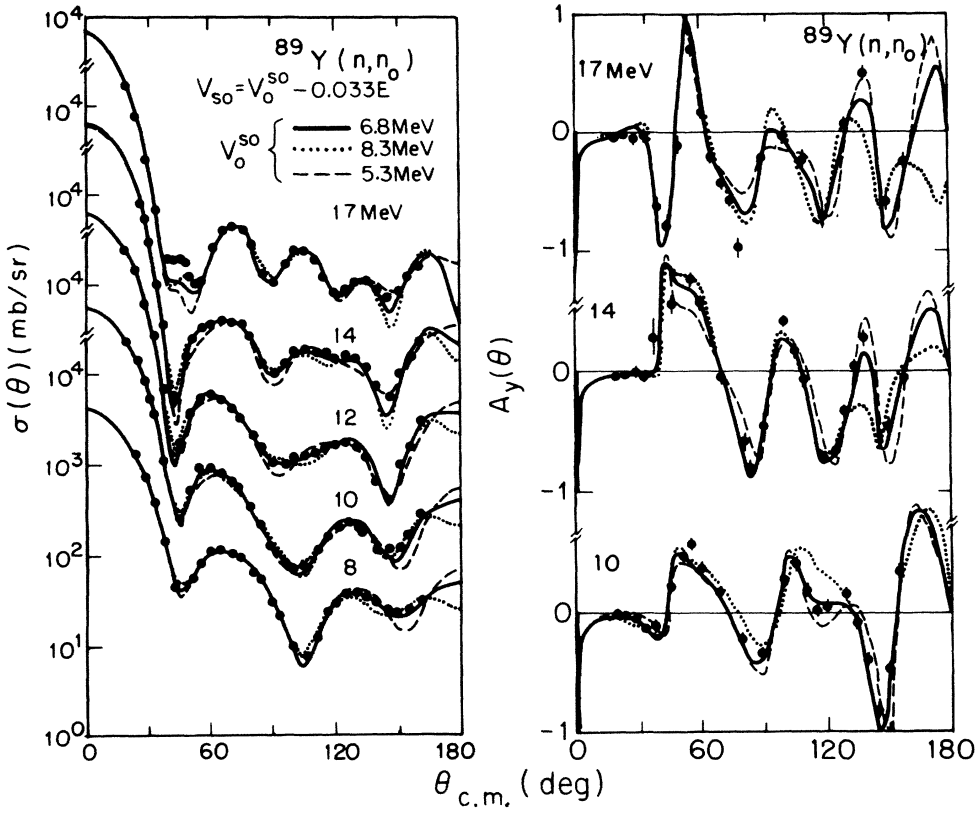

FIG. 6. Study of the sensitivity of spherical optical model calculations for ^{89}Y to the strength V_{SO} of the real spin-orbit potential. The data are from the present work.

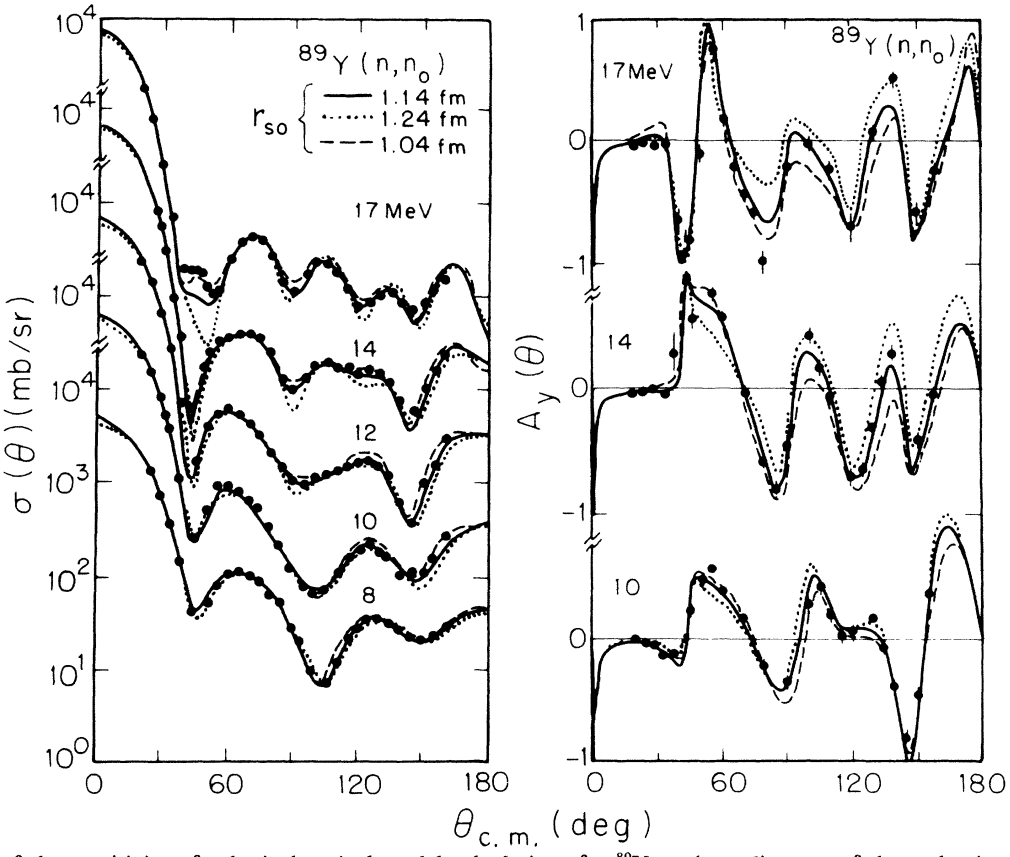

FIG. 7. Study of the sensitivity of spherical optical model calculations for ^{89}Y to the radius r_{SO} of the real spin-orbit potential. The data are from the present work.

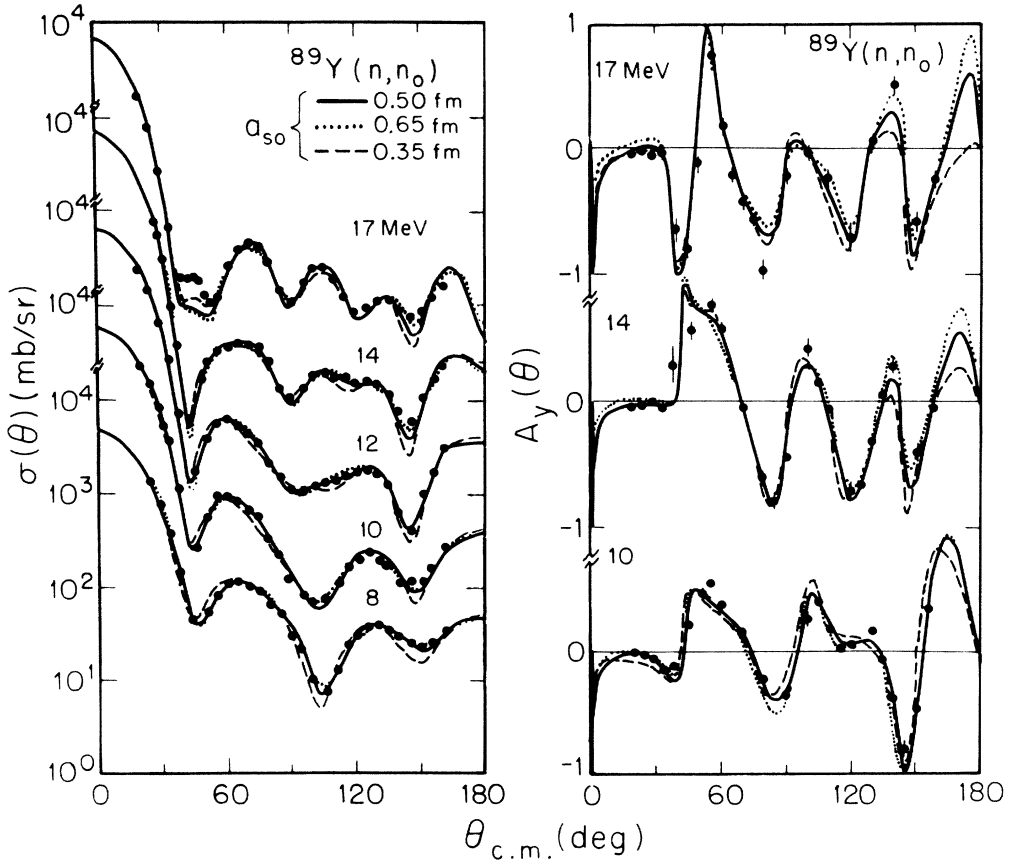

FIG. 8. Study of the sensitivity of spherical optical model calculations for ^{89}Y to the diffuseness a_{SO} of the real spin-orbit potential. The data are from the present work.

ter set. It was hoped that the demonstrated sensitivity to the spin-orbit radius might provide some means of improving the description of $\sigma(\theta)$; unfortunately, reducing r_{SO} to 1.04 fm had adverse effects on the predictions of analyzing power at 17 MeV and below, and so this approach was abandoned.

Our model also differs from that of RKF (and Becchetti and Greenlees and other classical SOM studies) in that it includes a complex spin-orbit term. No assumptions were made *a priori* about either the existence or the behavior of W_{SO}. In the past, since there have been no suitable $A_y(\theta)$ data and since $\sigma(\theta)$ is relatively insensitive to this term, it is usual to neglect it. It was not present in the starting parameter set[19] and was introduced into our model only after the initial optimization of all other parameters. The strength of W_{SO} was first included as a small positive constant ($W_{SO} \simeq 700$ keV), but it was later determined using the χ^2 criterion that a small decreasing variation with energy was preferred. We found, not surprisingly, that the analyzing power data were quite sensitive to the presence of W_{SO}, and we are able to noticeably improve our fits by including it. Tests of the correlation between W_{SO} and other SOM parameters indicate that fits of this quality are not possible without the inclusion of such a term.

Likewise, it was not explicitly required that the geometrical parameters of W_{SO} be the same as those of V_{SO}; rather, they were introduced into the model as identical and then varied to determine the actual best values. The search procedure, which was based on minimizing χ^2 over all distributions, led to values that are quite different from their real counterparts, but are qualitatively similar to those found in other TUNL studies of this potential.[24]

A sensitivity study for W_{SO}, similar to those described above for V_{SO}, is shown in Fig. 9. It is worth noting that for the range of W_{SO} values shown in this figure, the calculated value of $A_y(\theta)$ drops to a lower value throughout the entire angular range as the strength of W_{SO} increases. As can be seen by reference to Table I, our value of W_{SO} has the same sign as that of V_{SO}, a result that is at variance with nuclear model predictions,[25,26] but in agreement with TUNL results for other spherical and near-spherical nuclei.[3,27,28]

E. Calculations with existing global optical potentials

Since the data were represented so well by the energy-dependent model presented above, it was a point of interest to see how the data fit into a SOM of broader scope. Two such existing models were considered for this test:

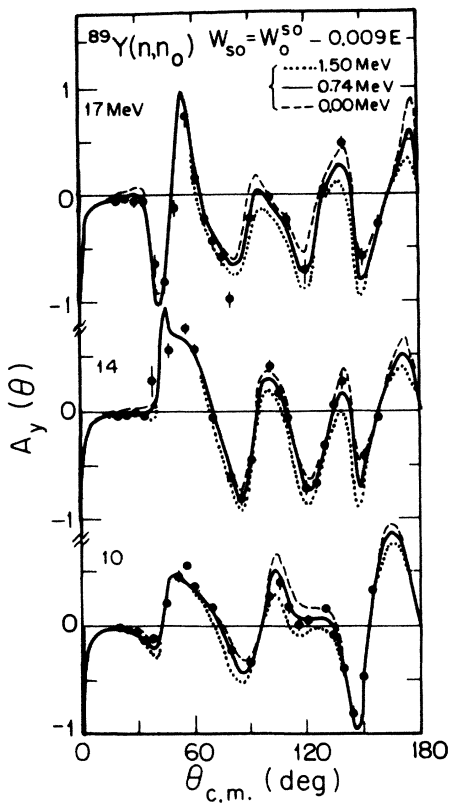

FIG. 9. Study of the sensitivity of spherical optical model calculations for ^{89}Y to the strength W_{SO} of the imaginary spin orbit potential. The solid and dotted curves are calculated with values of $W_0^{SO}=0.74$ and 1.50 MeV, respectively; the dashed curves are for $W_{SO}=0.0$. The data are from the present work.

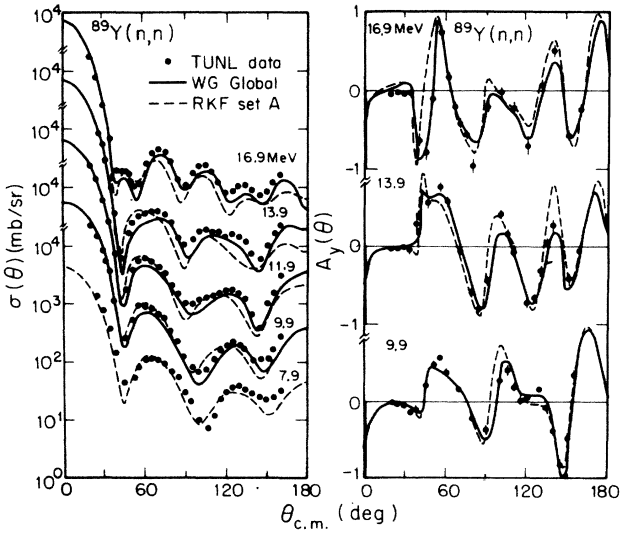

FIG. 10. Differential cross sections and analyzing powers for elastic scattering of neutrons from ^{89}Y. The solid curves are from calculations using the WG spherical optical model parameters, the dashed curves are calculated from the RKF parameters.

the global parameter set A of Rapaport, Kulkarni, and Finlay[2] and the Walter-Guss[3] set, developed at TUNL. Both parameter sets are based on extensive optical model searches of neutron cross section data for several spherical and deformed nuclei up to ^{208}Pb. However, the WG parameters are also based on searches of analyzing power data, from which the spin-orbit parameters are mainly derived; the RKF model uses the well-known values of Becchetti and Greenlees for the spin-orbit potential.[21] Furthermore, the WG model included the ^{89}Y data at 10, 14, and 17 MeV of the present paper in their global set, but with a reduced weighting relative to that of other sets. The optical model parameters of WG and RKF are compared to those of this work in Table I.

Calculations using the RKF and WG models are shown in Fig. 10. It is clear that the representation of $\sigma(\theta)$ by the RKF model is generally poor when compared to the data, having problems reproducing both the magnitude and the phasing of the angular distributions. What is then perhaps surprising is the quality of representation of the $A_y(\theta)$ data. If one compares the RKF calculations in these figures to those calculations in Fig. 4 from the present SOM analysis, one sees that the present representation of $\sigma(\theta)$ is vastly superior. In contrast, the RKF analyzing power representations appear qualitatively similar to those of the present work, yet the χ^2 values for the RKF calculations are about 50% larger.

Using the WG model, the agreement with the $\sigma(\theta)$ is much improved over the RKF calculations; however, the representation is still seriously flawed, particularly in the reproduction of the overall magnitudes of the $\sigma(\theta)$ data beyond 40°. The WG calculations of $A_y(\theta)$ are fairly good, roughly comparable to those using the RKF parameters, and nearly as good at those with the present ^{89}Y model. Calculations of the total cross sections for both models are listed in Table II. The WG set is in close agreement with the data and the values using the set derived here. The RKF calculations differ by as much as 8% at 8 MeV.

It is tempting to attribute these differences in representational ability to specific parts of the optical potentials. However, because the SOM parametrization is not unique and because the parameters are not all independent, this is difficult. One point that particularly deserves to be addressed is the question of differences in overall normalization of the $\sigma(\theta)$ curves. Although the normalizations of the measured $\sigma(\theta)$ data for ^{89}Y are self-consistent (and consistent with the normalization of the data of Hansen *et al.*), neither global model can account for what appears to be an anomalous normalization of the entire data set. We would like to demonstrate that this "anomaly" can be mostly accounted for in a simple way by varying the strength of the absorptive potential.

Starting with the existing WG parameters, we first allowed the magnitude of the surface absorptive potential W_d to vary in the search. The outcome was entirely expected: this data set prefers a "shallower" potential depth than had been indicated in the WG global searches over the entire data base. We searched next on the energy dependence (the slope α_d) of W_d, first alone, and then in

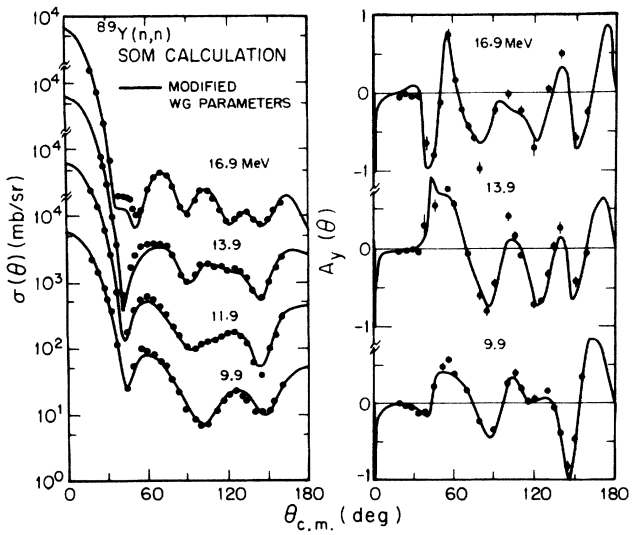

FIG. 11. Differential cross sections and analyzing powers for elastic scattering of neutrons from ^{89}Y. The solid curves are from calculations using the modified WG spherical optical model parameters.

conjunction with the magnitude (the intercept W_{0d}) of W_d. This search yielded a somewhat different slope and intercept for this energy dependence and the descriptions of $\sigma(\theta)$ and $A_y(\theta)$ were much improved, to the point of being almost as good as the specialized yttrium model. The calculations using the modified WG parameters are shown in Fig. 11. The values used here are $W_{0d}=7.480$ MeV and $\alpha_d=0.137$; these values represent significantly less absorption than in the original WG model and the model derived in the present paper; for instance, the corresponding values at $E=14$ MeV for W_d are 5.56, 6.80, and 6.56 MeV, respectively.

F. Extension to microscopic optical potentials

Microscopic models have been used to describe cross sections for neutron scattering between 4 and 17 MeV for Fe, Pb, and U in Refs. 29–32. Similar calculations have been performed at 14.6 MeV for a wide range of nuclei,[4] including ^{89}Y. An illustration of the calculations at 14.6 MeV for ^{89}Y(n,n$_0$) scattering is given in Ref. 4, where it is shown that the $\sigma(\theta)$ data can be well represented using central potentials calculated by the prescription of Jeukenne, Lejeune, and Mahaux (JLM).[32] The spin-orbit potential, taken to be real, was based on an effective interaction of Bertsch *et al.*[33] However, since no $A_y(\theta)$ data were available for ^{89}Y at the time of these calculations, no predictions of analyzing power were shown in the paper of Ref. 4. No statement can be made here regarding the possible success of microscopic calculations in describing the $A_y(\theta)$ data. However, it is clear that the data set for ^{89}Y reported in the present paper will be important for testing the ability of the microscopic calculations to describe this observable. A collaboration with the group at Livermore (L.H. and F.D.) is planned for extending the SOM analyses of the present ^{89}Y data into the area of microscopic potentials.

IV. SUMMARY

Differential cross sections and analyzing powers have been measured for the nucleus ^{89}Y in the energy range between 8 and 17 MeV. A description of the data has been made using the spherical optical model formalism; excellent results are achieved using a parameter set based on average geometries and linearly varying potential well strengths. A comparison to two existing global SOM parameter sets has also been made.

In the context of this analysis, the data indicate the need of an imaginary part of the spin-orbit potential. Our investigation confirms that this term is of a sign and magnitude comparable to values obtained in several earlier TUNL studies in this energy range.

This work was supported by the U.S. Department of Energy, Office of High Energy and Nuclear Physics, under Contract No. DE-AC05-76ER01067.

*Present address: Department of Radiology, Duke University Medical Center, Durham, NC 27710.

†Present address: Indiana University Cyclotron Facility, Bloomington, IN 47405.

‡Present address: Max-Planck-Institut für Kernphysik, Heidelberg, Federal Republic of Germany.

[1]J. Rapaport, Phys. Rep. **87**, 27 (1982).

[2]J. Rapaport, V. Kulkarni, and R. W. Finlay, Nucl. Phys. **A330**, 15 (1979).

[3]R. L. Walter, in *Neutron-Nucleus Collisions—A Probe of Nuclear Structure,* AIP Conf. Proc. No. 124, edited by J. Rapaport, R. W. Finlay, S. M. Grimes, and F. S. Dietrich (AIP, New York, 1985), p. 53.

[4]L. F. Hansen, F. S. Dietrich, B. A. Pohl, C. H. Poppe, and C. Wong, Phys. Rev. C **31**, 111 (1985).

[5]Yan Yiming, C. E. Brient, R. W. Finlay, G. Randers-Pehrson, A. Marcinkowski, R. C. Tailor, and J. Rapaport, Nucl. Phys. **A390**, 449 (1982).

[6]W. Benenson, S. M. Austin, R. A. Paddock, and W. G. Love, Phys. Rev. **176**, 1268 (1968).

[7]J. D. Vergados and T. T. S. Kuo, Nucl. Phys. **A168**, 225 (1971).

[8]P. Hoffman-Pinther and J. L. Adams, Nucl. Phys. **A229**, 365 (1974).

[9]K. Fujita and T. Komoda, Prog. Theor. Phys. **60**, 178 (1978).

[10]S. M. El-Kadi, C. E. Nelson, F. O. Purser, R. L. Walter, A. Beyerle, C. R. Gould, and L. W. Seagondollar, Nucl. Phys. **A390**, 509 (1982).

[11]W. Tornow, E. Woye, G. Mack, C. E. Floyd, K. Murphy, P. P. Guss, S. Wender, R. C. Byrd, R. L. Walter, and H. Leeb,

Nucl. Phys. **A385**, 376 (1982).
[12]J. C. Hopkins and G. Breit, Nucl. Data Tables A **9**, 137 (1971).
[13]G. G. Ohlsen, J. L. McKibben, G. P. Lawrence, P. W. Keaton, and D. D. Armstrong, Phys. Rev. Lett. **27**, 599 (1971).
[14]R. C. Byrd, P. W. Lisowski, W. Tornow, and R. L. Walter, Nucl. Phys. **A404**, 29 (1983); see also W. Haeberli, in *Fast Neutron Physics,* edited by J. B. Marion and J. L. Fowler (Wiley, New York, 1963), p. 1390.
[15]H. H. Hogue, computer code EFFIGY (unpublished).
[16]E. Woye, W. Tornow, G. Mack, C. E. Floyd, P. P. Guss, K. Murphy, R. C. Byrd, S. A. Wender, R. L. Walter, T. B. Clegg, and W. Wylie, Nucl. Phys. **A394**, 139 (1983).
[17]D. G. Foster, Jr. and D. W. Glasgow, Phys. Rev. C **3**, 576 (1971).
[18]C. E. Floyd, Jr., Ph.D. dissertation, Duke University, 1981.
[19]P. P. Guss, Ph.D. dissertation, Duke University, 1982.
[20]P. E. Hodgson, *Nuclear Reactions and Nuclear Structure* (Oxford University Press, Oxford, 1971).
[21]F. D. Becchetti and G. W. Greenlees, Phys. Rev. **182**, 1190 (1969).
[22]J. Schwinger, Phys. Rev. **73**, 407 (1948).
[23]Ph. Martin, private communication.
[24]R. L. Walter, W. Tornow, P. P. Guss, and J. P. Delaroche, in *Neutron-Nucleus Collisions—A Probe of Nuclear Structure,* Ref. 3, p. 312.
[25]B. C. Clark, S. Hama, and R. L. Mercer, in *The Interaction Between Medium Energy Nucleons in Nuclei—1982,* AIP Conf. Proc. No. 97, edited by H. O. Meyer (AIP, New York, 1982), p. 260.
[26]F. A. Brieva and J. R. Rook, Nucl. Phys. **A297**, 206 (1978).
[27]R. C. Byrd, P. W. Lisowski, W. Tornow, and R. L. Walter, Nucl. Phys. **A404**, 29 (1983).
[28]G. M. Honoré, W. Tornow, C. R. Howell, R. S. Pedroni, R. C. Byrd, R. L. Walter, and J. P. Delaroche, Phys. Rev. C **33**, 1129 (1986).
[29]S. Mellema, R. W. Finlay, F. S. Dietrich, and F. Petrovich, Phys. Rev. C **28**, 2267 (1983).
[30]J. R. M. Annand, R. W. Finlay, and F. S. Dietrich, Nucl. Phys. **A443**, 249 (1985).
[31]L. F. Hansen (unpublished).
[32]J. P. Jeukenne, A. Lejeune, and C. Mahaux, Phys. Rev. C **16**, 80 (1977).
[33]G. Bertsch, J. Borysowicz, H. McManus, and W. G. Love, Nucl. Phys. **A284**, 399 (1977).